Research article

# Liraglutide ameliorates TAC-induced cardiac hypertrophy and heart failure by upregulating expression level of ANP expression

Ruisha Li [a],[1], Keyin Zhang [a],[1], Zhenjun Xu [a], Yanrong Yu [b], Dongjin Wang [a], Kai Li [a],[***], Wenxue Liu [a],[*], Jun Pan [a],[**]

[a] *Institute of Cardiothoracic Vascular Disease, Department of Cardio-Thoracic Surgery, Nanjing Drum Tower Hospital, The Affiliated Hospital of Nanjing University Medical School, Nanjing, Jiangsu, China*
[b] *Department of Cardio-Thoracic Surgery, Nanjing Drum Tower Hospital Clinical College of Nanjing University of Chinese Medicine, Nanjing, Jiangsu, China*

ABSTRACT

Recent studies have underscored the cardioprotective properties of liraglutide. This research explores its impact on cardiac hypertrophy and heart failure following transverse aortic constriction (TAC). We found that liraglutide administration markedly ameliorated cardiac hypertrophy, fibrosis, and function. These benefits correlated with increased ANP expression and reduced activity in the calcineurin A/NFATc3 signaling pathway. Moreover, liraglutide mitigated ER stress and cardiomyocyte apoptosis, and enhanced autophagy. Notably, the positive effects of liraglutide diminished when co-administered with A71915, an ANP inhibitor, suggesting that ANP upregulation is critical to its cardioprotective mechanism.

## 1. Introduction

Heart failure, a persistent clinical syndrome characterized by the gradual deterioration of cardiac function, is the primary cause of morbidity and mortality worldwide [1]. Cardiac hypertrophy, an adaptive response in which cardiomyocytes thicken to cope with increased left ventricular wall stress, often occurs in individuals with chronic hypertension or aortic stenosis [2]. However, it is crucial to recognize that this compensated state is typically temporary. Persistent adverse conditions can lead to excessive cell enlargement, cardiomyocyte death, and impaired contraction, ultimately resulting in irreversible ventricular dilation and heart failure [3–5]. While treatments for cardiac hypertrophy, such as β-blockers, anti-hypertensive drugs, and angiotensin-converting enzyme inhibitors, are available, they mainly offer symptomatic relief [6]. Thus, there is an imperative need to deepen our understanding of the pathophysiological mechanisms underlying cardiac hypertrophy to advance the development of effective therapies.

Glucagon-like peptide-1 (GLP-1), produced by the L-type epithelial cells in the intestine, serves as an incretin and plays a vital role in regulating glucose levels and food intake. The endogenous form of GLP-1 has a short plasma half-life, rapidly degraded by the enzyme dipeptidyl peptidase-4 [7–9]. Liraglutide, a long-acting analog of human GLP-1, is predominantly used to treat type 2 diabetes mellitus (T2DM) [10]. Extensive research indicates that liraglutide exerts cardioprotective effects in both animals and patients, manifested by a reduced risk of cardiovascular events [11], regulation of blood pressure [12], preservation of vascular endothelial cell function [13], and attenuation of cardiomyocyte injury [14]. However, the specific impact of liraglutide on cardiac hypertrophy and heart failure, as well as the underlying mechanisms, remain elusive.

Atrial natriuretic peptide (ANP), a cardiac hormone within the natriuretic peptides (NPs) family, primarily exerts its effects through interaction with the natriuretic peptide receptor 1 (NPR1) [15,16]. It is well-established that ANP plays essential and diverse roles in the cardiovascular system via autocrine and paracrine mechanisms [17,18]. A critical function of ANP is its rapid secretion by cardiomyocytes in response to mechanical stress, which aids in limiting cardiac hypertrophy, fibrosis, remodeling, and dysfunction. Research involving genetic ablation of both ANP and Npr1 in mice has demonstrated that their absence intensifies cardiac hypertrophy and maladaptive remodeling under pressure overload [19–21], underscoring ANP's crucial role in regulating cardiac remodeling.

Previous research indicated that GLP-1 receptor activation enhances ANP expression by promoting the translocation of the Rap guanine nucleotide exchange factor Epac2 (Rapgef4) to the cell membrane [22]. This evidence leads to the hypothesis that liraglutide could play a protective role against cardiac hypertrophy and heart failure by modulating ANP expression. Our study aims to explore this hypothesis and investigate the associated mechanisms for the first time, both in vitro and in vivo.

## 2. Materials and methods

### 2.1. Animals and pressure overload model

Male C57BL/6J mice, aged 8–10 weeks, were acquired from GemPharmatech Company (Nanjing, Jiangsu). The experimental protocol received approval from Experimental Animal Ethics Committee of Drum Tower Hospital of Nanjing University Medical School. The mice were maintained in a controlled environment, observing a 12-h light/dark cycle, and had ad libitum access to food and water. The pressure overload model was established using a transverse aortic constriction (TAC) operation.

The mice were randomly allocated into three groups: 1) Sham group, where mice underwent the surgical procedure without aortic arch banding; 2) TAC group, where mice were subjected to the TAC operation; and 3) TAC + Liraglutide (Lira) group, where post-TAC, mice received daily intraperitoneal (i.p.) injections of liraglutide (HY–P0014, MCE) at a dose of 100 μg/kg for 4 weeks, a dosage determined from prior research [23] and our preliminary experiments (Sup. 1A - 1D). For the TAC operation, mice were anesthetized with isoflurane and placed in a supine position on a surgical platform. A median incision was made along the upper sternal segment to expose the aortic arch, followed by ligation between the right brachiocephalic and left common carotid artery using 6-0 silk suture around a 27-gauge needle, which was subsequently removed to achieve a defined aortic constriction. Cardiac function was assessed using a small Animal Ultrasound Imaging System (VEVO2100, FUJIFILM VISUALSONICS, Canada) by an investigator blinded to the group allocations.

### 2.2. Cell culture

The H9c2 cell line was sourced from the Cell Bank of the Chinese Academy of Sciences (Shanghai, China). These cells were cultured in high-glucose DMEM (319-005-CL, WISENT) supplemented with 10 % FBS (311-011-CL, WISENT) and 1 % penicillin-streptomycin (625-035-EG, WISENT) in an incubator maintained at 37 °C and 5 % CO2. The cells were stratified into four distinct groups: 1) Control (Con) group, where cells were treated with phosphate-buffered saline (PBS); 2) Isoprenaline (ISO) group, with cells exposed to ISO (100 nmol/L, 51-30-9, Aladdin) for 72 h to induce cardiomyocyte hypertrophy; 3) ISO + Lira group, where cells were co-incubated with ISO (100 nmol/L) and liraglutide (100 nmol/L, HY-P0014, MCE) to assess liraglutide's efficacy against ISO-induced cardiomyocyte hypertrophy; 4) ISO + Lira + A71915 group, involving cells pre-treated with A71915 (10 μmol/L, 132,956-87-7, Absin), a competitive ANP inhibitor, 3 h prior to ISO and liraglutide administration to elucidate ANP's pivotal role in liraglutide's cardioprotective action. The selection of dosages and treatment durations were guided by findings from prior research [24–27] and an initial experimental phase.

### 2.3. Western blotting

Protein was extracted from left ventricles or H9c2 cells using RIPA lysis buffer, which included proteinase and phosphatase inhibitors. Protein concentration was determined using the Pierce™ BCA Protein Assay Kit (23,225, Thermo) with a standardization to 1 μg/μL. For each analysis, 20 μg of protein was loaded per well, separated by SDS/PAGE electrophoresis, and subsequently transferred onto 0.2 μm PVDF membranes. The membranes were then blocked with 5 % nonfat dry milk for 1 h at room temperature. Following this, membranes were incubated overnight at 4 °C with primary antibodies, including GAPDH (1:2000, ab8245, Abcam), ANP (1:500, AP8534A, Abcepta), BNP (1:500, DF6902, Affinit), MYH7 (1:1000, sc-53089, Santa cruz), Col1a (1:1000, ab6308, Abcam), Col3a1 (1:1000, ab7778, Abcam), TGFβ (1:1000, ab215715, Abcam), Smad2/3 (1:500, A18674, ABclonal), p-Smad2/3 (1:500, AP1343, ABclonal), Epac2 (1:1000, sc-28326, Santa cruz), ATF4 (1:1000, sc-390,063, Santa cruz), ATF6 (1:1000, sc-166,659, Santa cruz), CHOP (1:1000, sc-7351, Santa cruz), p62 (1:1000, ab207305, Abacm), LC3B–I/II (1:1000, ab63817, Abacm), Bax (1:1000, ab32503, Abacm), Bcl-2 (1:200, 3498, CST), cleaved caspase3 (1:1000, 9664, CST), Lamin B1 (1:1000, 13,435, CST), NFATc3 (1:1000, sc-8405,

Santa cruz), and calcineurin A (1:1000, ab282104, Abacm). After incubation, membranes were washed thrice with TBST and incubated with the secondary antibody at room temperature for 1 h, followed by three additional TBST washes, and detection with ECL solution. Protein expression levels were quantified using Image J software. All the original images of Western blot data are referred to Sup. 7.

### 2.4. RNA extraction and real-time quantitative polymerase chain reaction (RT-qPCR)

Total RNA was extracted from the left ventricles using TRIzol (15596018, Invitrogen). From 1 μg of total RNA, cDNA was synthesized using HiScript III RT SuperMix for qPCR (R323-01, Vazyme). RT-qPCR was conducted with ChamQ Universal SYBR qPCR Master Mix (Q711-02, Vazyme) on a Step One qPCR system (LC480, Roche), following a program of 40 cycles at 95 °C for 10 s, 60 °C for 15 s, and 72 °C for 20 s. The primer sequences are detailed in Table 1. Data were reported as average relative mRNA levels per group, with relative expression calculated using the $2^{-\Delta\Delta Ct}$ method, subtracting the Ct value of GAPDH from that of the target gene.

### 2.5. ELISA analysis

ANP levels in mouse serum were quantified using the ANP ELISA kit (NBP2-66733, NOVUS) following the manufacturer's guidelines. Briefly, 50 μL of standard solution and samples were added to wells, immediately followed by 50 μL of Biotinylated Detection Ab solution. After a 45-min incubation at 37 °C, the wells were emptied and washed with 350 μL of wash buffer, soaking for 1–2 min, then decanted and dried on absorbent paper. This wash was repeated thrice. Subsequently, 100 μL of HRP Conjugate solution was added to each well and incubated for 30 min at 37 °C. Following five washes, 90 μL of Substrate Reagent was added to each well and incubated for about 15 min at 37 °C. The reaction was stopped with 50 μL of Stop Solution, and the optical density (OD value) at 450 nm was measured using a microplate reader (Thermo MultiskanGO, Thermo).

### 2.6. Immunofluorescence staining

Cells were fixed with 4 % paraformaldehyde (PFA) for 10 min, permeabilized with PBS containing 0.3 % Triton-X-100 for 5 min, and blocked with 10 % goat serum for 1 h at room temperature. Subsequently, they were incubated with NFATc3 antibody (1:50, sc-8405, Santa cruz) overnight at 4 °C. After washing thrice with PBS, the cells were incubated with Alexa 594-conjugated secondary antibody for 1 h at room temperature. Nuclei staining was performed using DAPI. Confocal microscopy (FV3000, Olympus) was utilized to capture the images, and Image J software assessed the fluorescence intensity.

### 2.7. IHC staining

Tissue samples were fixed in 4 % PFA for 48 h, dehydrated with 30 % sucrose, and embedded in OCT. These were then sectioned into 10 μm slices using a cryostat (CryoStar NX50, Thermo). The slices were permeabilized with PBS containing 0.3 % Triton-X-100 and blocked with 10 % goat serum. For IHC staining, after hydrogen peroxide treatment for 10 min, the slices were incubated with ANP antibodies (1:50, AP8534A, Abcepta) overnight at 4 °C, followed by incubation with biotinylated secondary antibodies for 1 h at room temperature and ABC solution for 30 min. Visualization was achieved with DAB solution application. Image J software quantified the tissue signal intensity.

### 2.8. Masson staining

Myocardial fibrosis was assessed using Masson's Trichrome Stain Kit (G1340, Solarbio). Tissue sections were incubated in Mordant Solution at 60 °C for 1 h and then washed under running water for 10 min. Celestite Blue Solution was applied to the sections for 2 min, followed by two brief rinses in deionized water for 30 s each. Mayer's Hematoxylin Solution was added to the sections for 2 min, succeeded by two brief rinses in deionized water for 30 s each. The sections were then treated with Acid Differentiation Solution for a few seconds and rinsed under running water for 10 min. Ponceau-Acid Fuchsin Solution was applied to the sections for 10 min,

**Table 1**
Primer sequences for qPCR.

| Gene | Forward Primer (5′-3′) | Reverse Primer (5′-3′) |
| --- | --- | --- |
| *M-Col1a* | CCTCAGGGTATTGCTGGACAAC | CAGAAGGACCTTGTTTGCCAGG |
| *M-Col3a1* | GAGGAATGGGTGGCTATCCG | TCGTCCAGGTCTTCCTGACT |
| *M-ANP* | GCTTCCAGGCCATATTGGAG | GGGGGCATGACCTCATCTT |
| *M-BNP* | GAGGTCACTCCTATCCTCTGG | GCCATTTCCTCCGACTTTTCTC |
| *M-MYH7* | ACTGTCAACACTAAGAGGGTCA | TTGGATGATTTGATCTTCCAGGG |
| *M-GAPDH* | ACTCCACTCACGGCAAATTC | TCTCCATGGTGGTGAAGACA |
| *Rat-ANP* | AAAGCAAACTGAGGGGCTCTGCTCG | TTCGGTACCGGAAGCTGTTGCA |
| *Rat-BNP* | TGCCCCAGATGATTCTGCTC | TGTAGGGGCCTTGGTCCTTTG |
| *Rat-MYH7* | AGTTCGGGCGAGTCAAAGATG | CAGGTTGTCTTGTTCCGCCT |
| *Rat-GAPDH* | ACTCTACCCACGGCAAGTTC | TGGGTTTCCCGTTGATGACC |

followed by two brief rinses with deionized water. After treating the sections with Phosphomolybdic Acid Solution for 10 min, they were directly stained with Aniline Blue Solution for 5 min without washing. The sections were rinsed in Acetic Acid working Solution, prepared by mixing Acetic Acid Solution with water at a 1:2 ratio, for several minutes. Subsequent quick dehydration was performed in 95 % ethanol, three times for 10 s each, followed by three rounds of dehydration in absolute ethanol for 10 s each. Clearing was conducted in xylene, three times for 2 min each. Sections were sealed with resinize. Image J software quantified the extent of myocardial fibrosis.

### 2.9. Hematoxylin-eosin staining

Frozen sections were rinsed three times with ddH2O, then stained with hematoxylin solution for 2 min, followed by a quick dip in 1 % hydrochloric acid in alcohol and another rinse in ddH2O. Subsequently, the sections were stained with eosin solution for 1 min and rinsed again with ddH2O. Post-rinsing, sections were dehydrated using an alcohol gradient and cleared with xylene. Finally, the sections were mounted using a mounting medium.
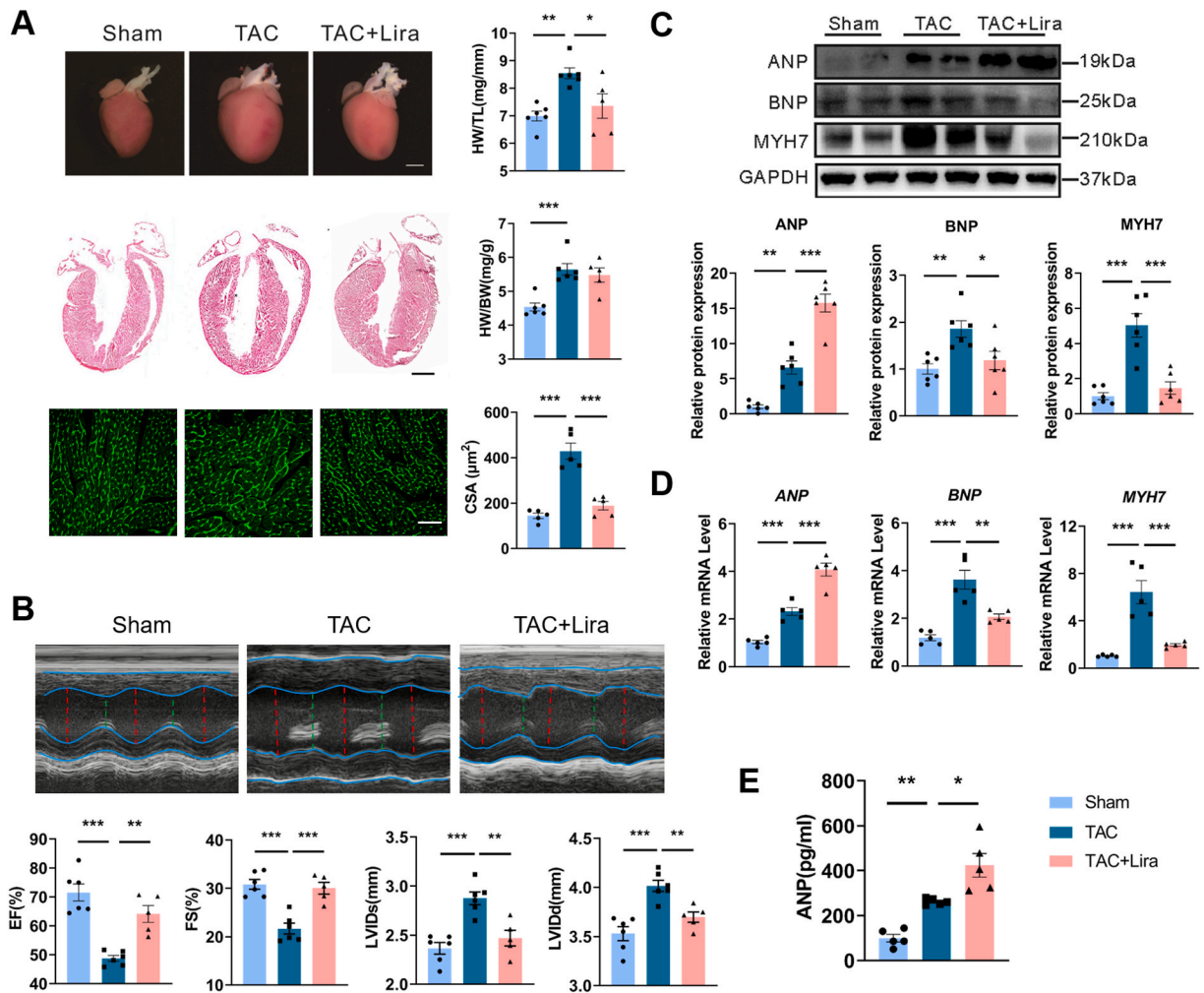


**Fig. 1.** Liraglutide alleviates transverse aortic constriction (TAC)-induced cardiac hypertrophy and heart failure, accompanied by substantial upregulation of ANP expression and release. A, Representative images of gross morphology of hearts (scale bar is 2 mm), hematoxylin-eosin (HE) staining (scale bar is 1 mm), wheat germ agglutinin (WGA) staining (scale bar is 50 μm), heart weight/tibia length (HW/TL) ratio, heart weight/body weight (HW/BW) ratio, and quantification of the cross-sectional area (CSA) of the hearts from the Sham, TAC, and TAC + Liraglutide (Lira) groups at 4 weeks after TAC (n = 5–6 per group). **B,** Echocardiographic analyses of cardiac function, including ejection fraction (EF), fractional shortening (FS), left ventricular internal diameter end systole (LVIDs) and left ventricular internal diameter end diastole (LVIDd) of the hearts from indicated groups (n = 5–6 per group). **C,** Western blot analyses and quantification of atrial natriuretic peptide (ANP), brain natriuretic peptide (BNP), and myosin heavy polypeptide 7 (MYH7) protein levels of the hearts form indicated groups (n = 6 per group). **D,** Real-time quantitative polymerase chain reaction (RT-qPCR) analyses and quantification of *ANP, BNP,* and *MYH7* mRNA levels of the hearts from indicated groups (n = 5 per group). **E,** ELISA analyses of serum ANP levels of the mice from indicated groups (n = 5 per group). $*P < 0.05$, $**P < 0.01$, $***P < 0.001$.

## 2.10. TUNEL assays

Apoptosis was identified using the One Step TUNEL Apoptosis Assay Kit (C1086, Beyotime). The sections were washed twice with PBS and incubated with 0.3 % Triton X-100 solution for 5 min at room temperature, followed by two PBS washes. TUNEL reaction solution was prepared and 50 μL was applied to each section, which was then incubated at 37 °C for 60 min. After three PBS washes, an anti-fade mounting medium was applied before imaging with a confocal microscope at 450–500 nm. Image J software was utilized to quantify the number of apoptotic cells based on staining.

## 2.11. Isolation of nuclear and cytoplasmic protein

Nuclear and cytoplasmic proteins were isolated using a Nuclear and Cytoplasmic Protein Extraction Kit (P0027, C1086, Beyotime). The cells were washed with PBS and detached using a cell scraper. For every 20 μL of cell pellet, 200 μL of cytoplasmic protein extraction reagent A with PMSF was added. After vortexing for 5 s, ensuring the cell pellet was fully resuspended, the mixture was placed in an ice bath for 15 min. Subsequently, 10 μL of cytoplasmic protein extraction reagent B was added, followed by vortexing for 5 s and an ice bath for 1 min. Centrifugation at 4 °C and 12,000 g for 5 min allowed for the extraction of cytoplasmic protein from the supernatant. After completely removing the supernatant, 50 μL of nuclear protein extraction reagent with PMSF was added to the pellet. The pellet was vortexed for 30 s, resuspended, and placed in an ice bath for 2 min, a process that lasted for 30 min. After centrifugation at 4 °C and 12,000 g for 10 min, the supernatant containing the nuclear protein was collected.
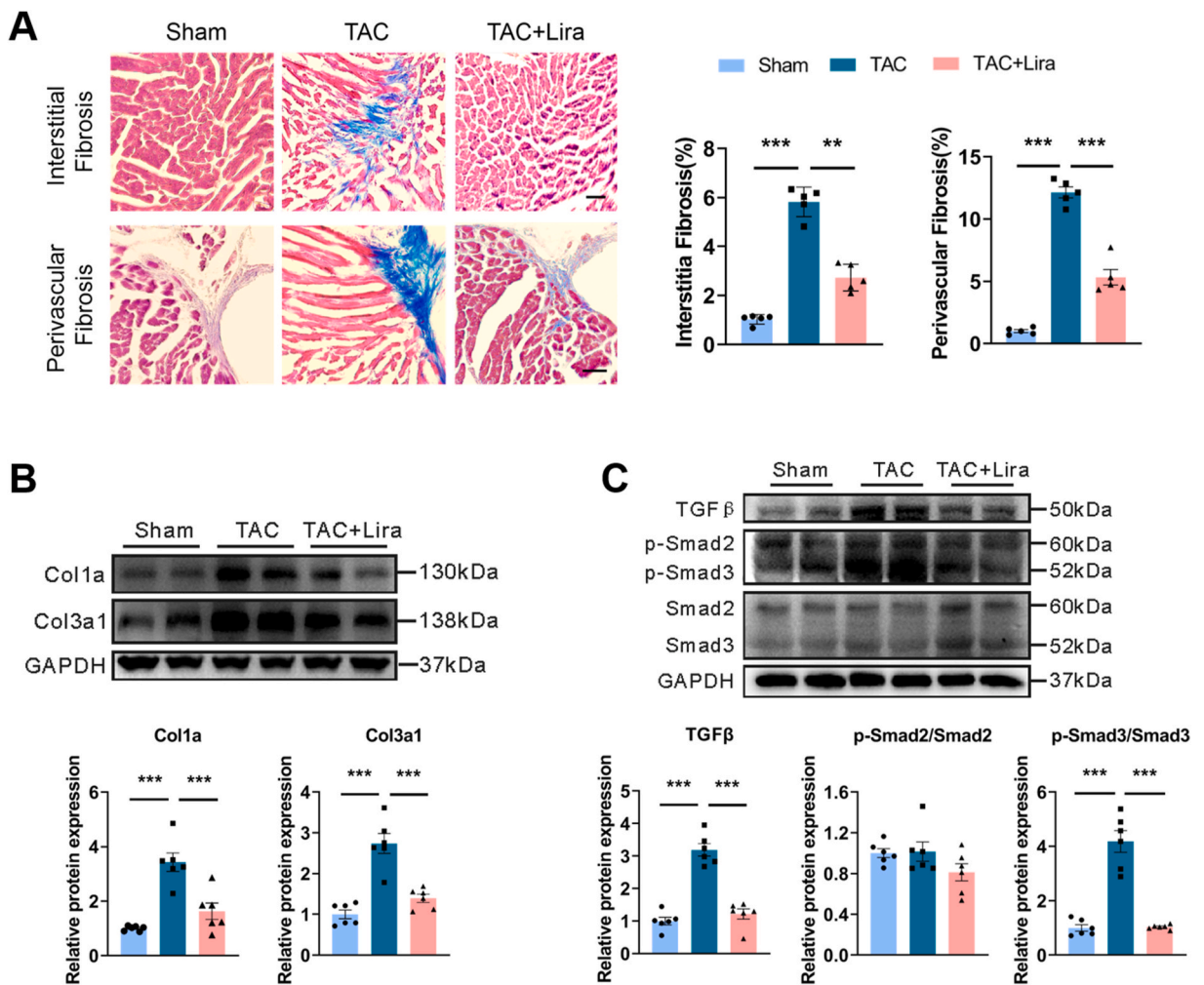


**Fig. 2.** Liraglutide mitigates TAC-induced cardiac fibrosis by downregulating the TGFβ-Smad3 signaling pathway. A, Representative Masson staining images of heart sections from mice in the Sham, TAC, and TAC + Lira groups at 4 weeks after TAC (Scale bar is 50 μm, n = 5 per group). **B,** Western blot analyses and quantification of Col1a and Col3a1 protein levels of the hearts from indicated groups (n = 6 per group). **C,** Western blot analyses and quantification of TGFβ, *p*-Smad2, Smad2, *p*-Smad3, and Smad3 protein levels of the hearts from indicated groups (n = 6 per group). *$P < 0.05$, **$P < 0.01$, ***$P < 0.001$.

For fresh tissue, it was first ground into powder, then 20 μL of the tissue was treated with reagent A, followed by the same steps as the cell isolation process.

## 2.12. Statistical analysis

Data were presented as means ± S.E.M. Statistical analyses were conducted using an unpaired *t*-test to assess the significance between two groups or one-way ANOVA followed by Tukey's post hoc test for multiple comparisons. GraphPad Prism 9.0 (GraphPad Software, CA) was utilized for data analysis and figure generation. A significance level of $P < 0.05$ was deemed statistically significant.

## 3. Results

### 3.1. Liraglutide mitigates TAC-induced cardiac hypertrophy and heart failure with significant upregulation of ANP expression and release

We initially investigated the impact of various liraglutide doses (25, 50, 100, and 200 μg/kg) administered once daily for 4 weeks on TAC-induced cardiac dysfunction. Notably, doses of 100 μg/kg and 200 μg/kg markedly improved cardiac function post-TAC surgery (Sup. 1A – 1C). Based on these findings, a dose of 100 μg/kg was selected for further exploration of the mechanisms involved.

Subsequent experiments revealed that, compared to the Sham group, the TAC group exhibited a significant increase in heart weight
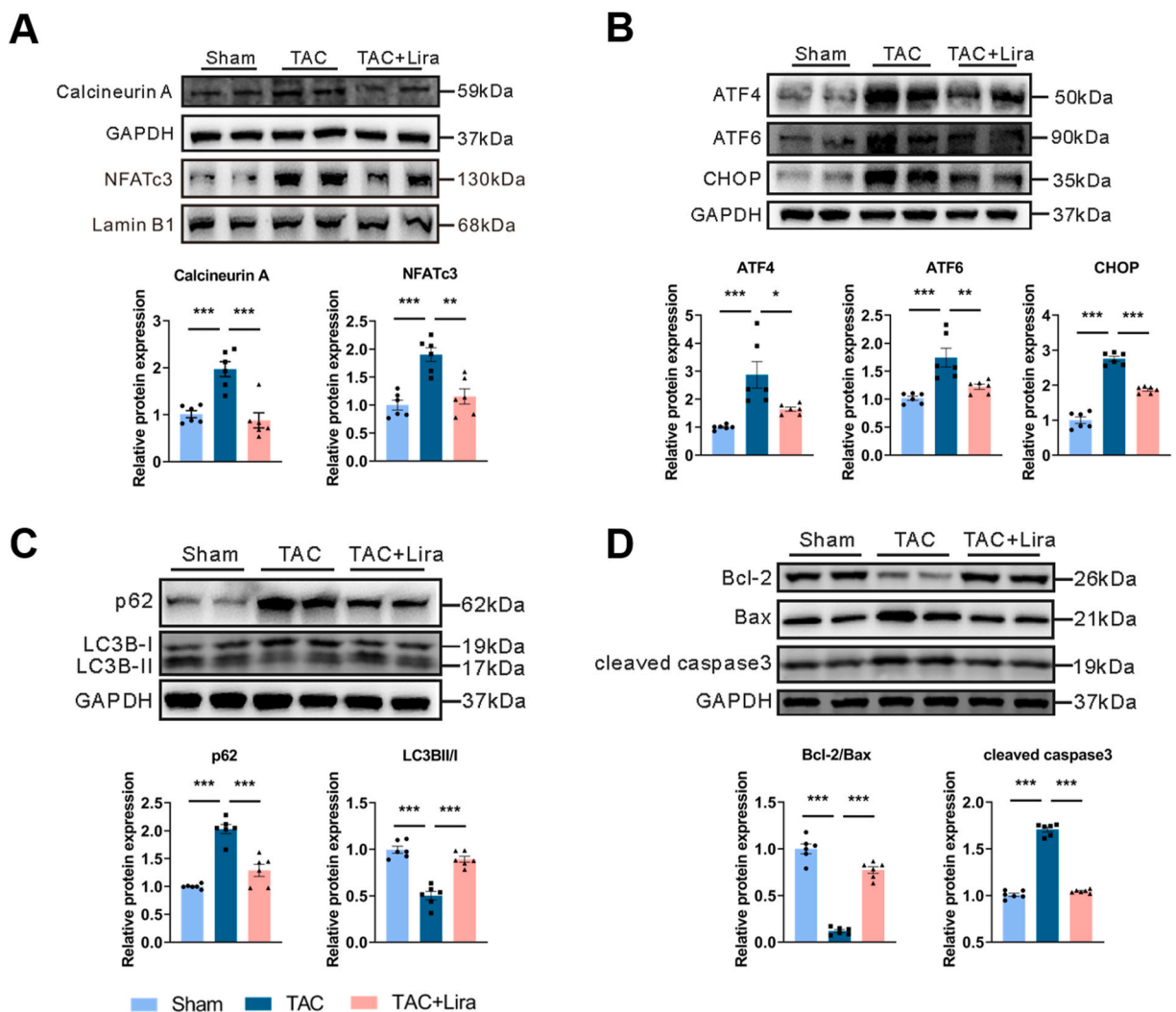


**Fig. 3.** Inhibition of the calcineurin A/NFATc3 signaling pathway, ER stress, and myocardial apoptosis, enhancing autophagy is involved in the protective role of liraglutide against TAC-induced cardiac hypertrophy and heart failure. Western blot analyses and quantification of calcineurin A, NFATc3 (**A**), ATF4, ATF6, CHOP (**B**), p62, LC3B–I/II (**C**), Bcl-2, Bax and cleaved caspase3 (**D**) protein levels of the hearts from indicated groups (n = 6 per group). *$P < 0.05$, **$P < 0.01$, ***$P < 0.001$.

(HW)/tibal length (TL) ratio, HW/body weight (BW) ratio, and cardiomyocyte area (Fig. 1A). There was also a significant reduction in ejection fraction (EF) and fractional shortening (FS) (Fig. 1B). Additionally, there was an obivous increasing in left ventricular internal diameter end systole (LVIDs) and left ventricular internal diameter end diastole (LVIDd) (Fig. 1B). We also assessed changes in hypertrophic markers. The TAC group showed a notable increase in ANP, brain natriuretic peptide (BNP), and β-myosin heavy chain (MYH7) levels (Fig. 1C and D). However, liraglutide treatment reduced mRNA and protein levels of BNP and MYH7 (Fig. 1C and D), while significantly elevating ANP levels in the left ventricle (Fig. 1C and D and Sup. 2A) and serum (Fig. 1E). These results indicate that liraglutide effectively counteracts pressure overload-induced cardiac hypertrophy and heart failure, potentially through the upregulation of ANP. Intriguingly, liraglutide did not affect the HW to BW ratio (Fig. 1A), a phenomenon possibly linked to the weight loss induced by liraglutide (Sup. 2B).

### 3.2. Liraglutide attenuates TAC-induced cardiac fibrosis by inhibiting the TGFβ-Smad3 signaling pathway

We further assessed the effect of liraglutide on cardiac fibrosis, a prevalent accompanying feature of cardiac hypertrophy and heart failure. When comparing the TAC group to the Sham group, a significant increase in interstitial and perivascular fibrosis was observed (Fig. 2A), along with the upregulation of collagen genes and the collagen proteins Col1a and Col3a1 (Fig. 2B, Sup. 3). This was associated with elevated expression levels of TGFβ and p-Smad3/Smad3, with no changes detected in p-Smad2/Smad2 (Fig. 2C).
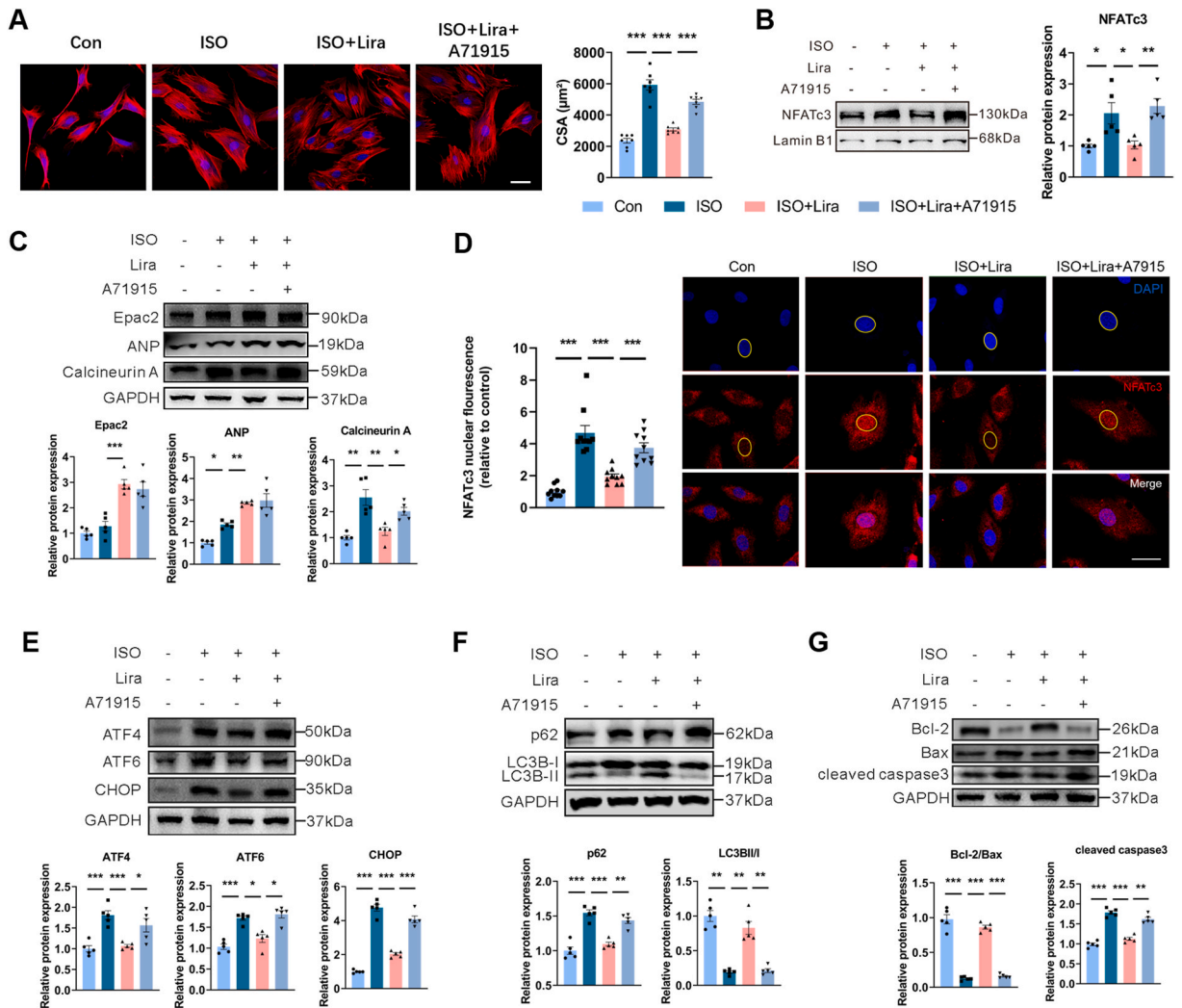


**Fig. 4.** Administration of A71915, an ANP competitive inhibitor, diminished the protective role of liraglutide in vitro. A, Representative images of H9c2 sections stained with phalloidine (scale bar is 50 μm) and the quantification of the CSA of the cells from indicated groups (n = 7 per group). Western blot analyses and quantification of NFATc3 (**B**), Epac2, ANP, and calcineurin A (**C**) protein levels of the hearts from indicated groups (n = 5 per group). **D**, Immunofluorescence staining analyses and quantification of NFATc3 in the nucleus of H9c2 cells from indicated groups (Scale bar is 50 μm, n = 10 per group). Western blot analyses and quantification of ATF4, ATF6, CHOP (**E**), p62, LC3B–I/II (**F**), Bcl-2, Bax, and cleaved caspase3 (**G**) protein levels of the H9c2 cells from indicated groups (n = 5 per group). *$P < 0.05$, **$P < 0.01$, ***$P < 0.001$.

Liraglutide administration significantly reversed these changes, suggesting its efficacy in mitigating myocardial fibrosis through modulating the TGFβ-Smad3 pathway, rather than the Smad2 pathway.

### 3.3. Liraglutide's protective role against TAC-induced cardiac hypertrophy and heart failure involves inhibition of the calcineurin A/ NFATc3 pathway, ER stress, and myocardial apoptosis, and enhancement of autophagy

The calcineurin A/NFATc3 signaling pathway, ER stress, autophagy, and apoptosis are pivotal in the progression of cardiac hypertrophy and heart failure. Therefore, we explored liraglutide's effects on these processes. Our findings indicated that TAC significantly upregulated calcineurin A, enhanced NFATc3 nuclear translocation (Fig. 3A), activated ER stress (as shown by increased ATF4, ATF6, CHOP) (Fig. 3B), and triggered apoptosis (demonstrated by an elevated Bcl2/Bax ratio, increased cleaved caspase 3 levels, and TUNEL-positive cells) (Fig. 3D and Sup. 4). Moreover, TAC suppressed autophagy, evidenced by the downregulation of LC3B II/I and the upregulation of p62 (Fig. 3C). Remarkably, liraglutide administration mitigated these effects, underscoring its potential in modulating key pathways to improve cardiac hypertrophy and prevent heart failure.

### 3.4. Administration of A71915, an ANP competitive inhibitor, diminished the protective role of liraglutide in vitro

We explored the crucial role of ANP upregulation in liraglutide's protective effects against cardiac hypertrophy and heart failure using an ISO-induced hypertrophy model in H9c2 cells. Initially, we assessed the impact of varying liraglutide concentrations (1, 10, 100, and 1000 nM) on ISO-induced cellular hypertrophy, as previously documented [27]. Findings in Sup. 5 revealed that liraglutide at 100 nM and 1000 nM concentrations notably reduced ISO-induced cellular hypertrophy. Therefore, we selected 100 nM for further experiments. Subsequent studies showed ISO-induced activation of calcineurin A (Fig. 4C) and NFATc3 nuclear translocation (Fig. 4B and D), which led to the upregulation of cardiac hypertrophy markers (such as ANP and BNP) in mRNA and protein levels (Fig. 4C, Sup.6A and B) and cellular enlargement (Fig. 4A). ISO treatment also increased ER stress markers (ATF4, ATF6, and CHOP) (Fig. 4E), apoptosis (evidenced by a higher Bcl2/Bax ratio and cleaved caspase 3) (Fig. 4G), and decreased autophagy (indicated by reduced LC3B II/I and increased p62 levels) (Fig. 4F). Liraglutide administration reversed these changes and further elevated ANP expression, attributed to Epac2 upregulation. However, pre-treatment with A71915, an ANP competitive inhibitor, reduced liraglutide's protective effects without affecting Epac2 or ANP expression, underscoring the vital role of ANP upregulation in liraglutide's cardioprotective mechanisms.

## 4. Discussion

Cardiac hypertrophy is a critical adaptive response of cardiomyocytes to pressure overload-induced mechanical stress, initially aiding in increasing cardiac output. However, chronic mechanical stress may lead to heart failure [28,29]. In our research, we have demonstrated for the first time that liraglutide's cardioprotective effects against cardiac hypertrophy and heart failure are significantly associated with the inhibition of the calcineurin A/NFATc3c signaling pathway, reduction of ER stress and apoptosis, and enhancement of autophagy, all facilitated by ANP upregulation.

Calcineurin is a serine/threonine-specific phosphatase activated by prolonged increases in intracellular calcium [30,31]. The active calcineurin complex comprises a 59- to 63-kDa catalytic subunit, calcineurin A, a 19-kDa calcium-binding subunit, calcineurin B, and calmodulin [32]. The nuclear factor of activated T cells (NFAT) is a transcription factor family with five identified members [33], among which NFATc3's activity is notably regulated by calcineurin A via dephosphorylation, facilitating its nuclear translocation, a process crucial in cardiac hypertrophy development [34,35]. The effect of liraglutide on this pathway was previously unexplored. Our findings reveal that liraglutide substantially attenuates calcineurin A/NFATc3 signaling in both in vivo and in vitro settings. Intriguingly, A71915, an ANP inhibitor, mitigated these effects in vitro, indicating that liraglutide modulates calcineurin A/NFATc3 signaling predominantly through ANP upregulation.

The endoplasmic reticulum (ER) plays a pivotal role in intracellular protein synthesis, folding, translocation, and calcium homeostasis [36]. Emerging research indicates that various stressors, including pressure overload, oxidative stress, hypoxia, and genetic mutations, can impair protein folding within the ER, thereby inducing ER stress [37]. This stress, when prolonged or severe, is recognized for leading to cell apoptosis, cardiac hypertrophy, and ultimately heart failure [38]. Furthermore, autophagy is essential for maintaining cardiovascular homeostasis and adapting to stress [39], serving as an intracellular process for degrading aged or damaged cytoplasmic components, such as dysfunctional organelles and misfolded proteins [40]. Evidence has shown that activating autophagy mitigates cardiac remodeling and dysfunction [41,42]. Accumulating research supports that sustained ER stress combined with suppressed autophagy contributes to cardiomyocyte apoptosis and advances the progression from cardiac hypertrophy to heart failure [43–45]. In our study, we observed that liraglutide primarily exerts a cardiac protective effect by diminishing ER stress and boosting autophagy, thereby preventing apoptosis. The beneficial outcomes are largely due to the upregulation of ANP.

ANP, a key natriuretic peptide synthesized mainly in the heart, has been extensively studied over recent decades [15]. Its diverse physiological impacts on the cardiovascular and renal systems, including natriuresis, diuresis, vasorelaxation, reduction of blood volume, and inhibition of the renin-angiotensin-aldosterone system (RAAS), have been elucidated [46]. The modulation of ANP levels and activity has recently become a focal point in clinical research, presenting promising therapeutic avenues for heart failure [46,47]. Our findings highlight the significant role of ANP upregulation and its influence on balancing ER stress and autophagy in the cardiac protective effects of liraglutide administration.

Our study offers significant insights into the molecular mechanisms contributing to the cardioprotective effects of liraglutide and

could facilitate the development of innovative treatments focused on ANP regulation. However, we recognize certain limitations in our research. Firstly, employing the H9C2 rat cardiomyocyte line instead of primary cultured cardiomyocytes may not capture the full complexity of the in vivo environment or precisely mimic the behavior of primary cardiomyocytes, which could influence the generality of our conclusions. Secondly, our exclusive use of isoproterenol (ISO) to induce cardiomyocyte hypertrophy might limit the applicability of our findings to other models of drug-induced cardiomyocyte hypertrophy, such as those induced by angiotensin II or phenylephrine. Future studies that involve primary cultured cardiomyocytes and a broader range of hypertrophic stimuli are essential to validate our findings and provide more comprehensive insights.

## 5. Conclusions

Our results indicate that liraglutide successfully attenuated cardiac hypertrophy and heart failure triggered by PO through the upregulation of ANP protein levels. Furthermore, liraglutide demonstrates considerable promise as a new therapeutic option for the management of cardiac hypertrophy and heart failure. However, further preclinical and clinical studies are needed to confirm these findings and solidify its therapeutic potential.

## Funding

## Code availability

Not applicable.

## Ethics declarations

All experimental procedures conducted in this study were approved by Experimental Animal Ethics Committee of Drum Tower Hospital of Nanjing University Medical School. Additionally, our study fully adheres to the Cell Press Editorial Ethics policies and Elsevier's Publishing Ethics policies.

## Consent to participate

Not applicable.

## Consent for publication

Not applicable.

## Data availability statement

Data are available from the corresponding author on reasonable request.

## CRediT authorship contribution statement

**Ruisha Li:** Methodology, Investigation, Formal analysis, Data curation. **Keyin Zhang:** Methodology, Investigation, Data curation. **Zhenjun Xu:** Methodology, Formal analysis. **Yanrong Yu:** Investigation, Data curation. **Dongjin Wang:** Funding acquisition, Conceptualization. **Kai Li:** Methodology, Formal analysis. **Wenxue Liu:** Writing – review & editing, Writing – original draft, Project administration, Methodology, Conceptualization. **Jun Pan:** Supervision, Methodology, Conceptualization.

## Declaration of competing interest

The authors declare the following financial interests/personal relationships which may be considered as potential competing interests: Dongjin Wang reports financial support was provided by National Natural Science Foundation of China. Wenxue Liu reports financial support was provided by National Natural Science Foundation of China. Jun Pan reports financial support was provided by National Natural Science Foundation of China. If there are other authors, they declare that they have no known competing financial interests or personal relationships that could have appeared to influence the work reported in this paper.

## Appendix A. Supplementary data

Supplementary data to this article can be found online at https://doi.org/10.1016/j.heliyon.2024.e32229.

## References

[1] T.G. Martin, M.A. Juarros, L.A. Leinwand, Regression of cardiac hypertrophy in health and disease: mechanisms and therapeutic potential, Nat. Rev. Cardiol. 20 (5) (2023) 347–363.

[2] R. Kamel, et al., Cyclic nucleotide phosphodiesterases as therapeutic targets in cardiac hypertrophy and heart failure, Nat. Rev. Cardiol. 20 (2) (2023) 90–108.

[3] J. Guo, et al., Canopy 2 attenuates the transition from compensatory hypertrophy to dilated heart failure in hypertrophic cardiomyopathy, Eur. Heart J. 36 (37) (2015) 2530–2540.

[4] M. Gao, et al., Isoliquiritigenin attenuates pathological cardiac hypertrophy via regulating AMPKα in vivo and in vitro, J. Mol. Histol. 53 (4) (2022) 679–689.

[5] T. Kou, et al., Effects of berberine hydrochloride on left ventricular structure and function in rats with myocardial hypertrophy, Acta Cardiol. 78 (4) (2023) 433–441.

[6] E.J. Benjamin, et al., Heart disease and stroke statistics-2018 update: a report from the American heart association, Circulation 137 (12) (2018) e67–e492.

[7] K. Pabreja, et al., Molecular mechanisms underlying physiological and receptor pleiotropic effects mediated by GLP-1R activation, Br. J. Pharmacol. 171 (5) (2014) 1114–1128.

[8] D.J. Drucker, M.A. Nauck, The incretin system: glucagon-like peptide-1 receptor agonists and dipeptidyl peptidase-4 inhibitors in type 2 diabetes, Lancet 368 (9548) (2006) 1696–1705.

[9] C. Rutledge, et al., Liraglutide Protects against Diastolic Dysfunction and Improves Ventricular Protein Translation, 2023.

[10] R. Pratley, et al., Oral semaglutide versus subcutaneous liraglutide and placebo in type 2 diabetes (PIONEER 4): a randomised, double-blind, phase 3a trial, Lancet 394 (10192) (2019) 39–50.

[11] S.P. Marso, et al., Liraglutide and cardiovascular outcomes in type 2 diabetes, N. Engl. J. Med. 375 (4) (2016) 311–322.

[12] I.H. Zucker, H.J. Wang, H.D. Schultz, GLP-1 (Glucagon-Like peptide-1) plays a role in carotid chemoreceptor-mediated sympathoexcitation and hypertension, Circ. Res. 130 (5) (2022) 708–710.

[13] E. Osto, et al., Rapid and body weight-independent improvement of endothelial and high-density lipoprotein function after Roux-en-Y gastric bypass: role of glucagon-like peptide-1, Circulation 131 (10) (2015) 871–881.

[14] M.H. Noyan-Ashraf, et al., A glucagon-like peptide-1 analog reverses the molecular pathology and cardiac dysfunction of a mouse model of obesity, Circulation 127 (1) (2013) 74–85.

[15] M. Forte, et al., NPPA/atrial natriuretic peptide is an extracellular modulator of autophagy in the heart, Autophagy 19 (4) (2023) 1087–1099.

[16] A. Aleksova, et al., Effects of Candesartan on Left Ventricular Function, Aldosterone and BNP in Chronic Heart Failure 26 (6) (2012) 131–143.

[17] T. Nishikimi, N. Maeda, H. Matsuoka, The role of natriuretic peptides in cardioprotection, Cardiovasc. Res. 69 (2) (2006) 318–328.

[18] M. Forte, et al., Cardiovascular pleiotropic effects of natriuretic peptides, Int. J. Mol. Sci. 20 (16) (2019).

[19] J.A. Feng, et al., Pressure-independent enhancement of cardiac hypertrophy in atrial natriuretic peptide-deficient mice, Clin. Exp. Pharmacol. Physiol. 30 (5–6) (2003) 343–349.

[20] T. Mori, et al., Volume overload results in exaggerated cardiac hypertrophy in the atrial natriuretic peptide knockout mouse, Cardiovasc. Res. 61 (4) (2004) 771–779.

[21] I. Kishimoto, K. Rossi, D.L. Garbers, A genetic model provides evidence that the receptor for atrial natriuretic peptide (guanylyl cyclase-A) inhibits cardiac ventricular myocyte hypertrophy, Proc. Natl. Acad. Sci. U. S. A. 98 (5) (2001) 2703–2706.

[22] M. Kim, et al., GLP-1 receptor activation and Epac2 link atrial natriuretic peptide secretion to control of blood pressure, Nat. Med. 19 (5) (2013) 567–575.

[23] Y. He, et al., The preventive effect of liraglutide on the lipotoxic liver injury via increasing autophagy, Ann. Hepatol. 19 (1) (2020) 44–52.

[24] K.R. Chaudhary, et al., Role of B-type natriuretic peptide in epoxyeicosatrienoic acid-mediated improved post-ischaemic recovery of heart contractile function, Cardiovasc. Res. 83 (2) (2009) 362–370.

[25] R. Li, et al., The glp-1 analog liraglutide protects against angiotensin II and pressure overload-induced cardiac hypertrophy via PI3K/Akt 1 and AMPKa signaling, Front. Pharmacol. 10 (2019) 537.

[26] Y. Yang, et al., Oxytocin protects against isoproterenol-induced cardiac hypertrophy by inhibiting PI3K/AKT pathway via a lncRNA GAS5/miR-375-3p/KLF4-dependent mechanism, Front. Pharmacol. 12 (2021) 766024.

[27] L. Huang, et al., Liraglutide suppresses production of extracellular matrix proteins and ameliorates renal injury of diabetic nephropathy by enhancing Wnt/β-catenin signaling, Am. J. Physiol. Ren. Physiol. 319 (3) (2020) F458–f468.

[28] G.B. Lim, Piezo 1 senses pressure overload and initiates cardiac hypertrophy, Nat. Rev. Cardiol. 19 (8) (2022) 503.

[29] S. Tual-Chalot, K. Stellos, Drug repurposing to prevent pressure overload-induced cardiac hypertrophy and heart failure, Eur. Heart J. 42 (36) (2021) 3783–3785.

[30] G.R. Crabtree, Generic signals and specific outcomes: signaling through Ca2+, calcineurin, and NF-AT, Cell 96 (5) (1999) 611–614.

[31] R.E. Dolmetsch, et al., Differential activation of transcription factors induced by Ca2+ response amplitude and duration, Nature 386 (6627) (1997) 855–858.

[32] J.D. Molkentin, Calcineurin and beyond: cardiac hypertrophic signaling, Circ. Res. 87 (9) (2000) 731–738.

[33] A. Rao, C. Luo, P.G. Hogan, Transcription factors of the NFAT family: regulation and function, Annu. Rev. Immunol. 15 (1997) 707–747.

[34] Z. Lin, et al., miR-23a functions downstream of NFATc3 to regulate cardiac hypertrophy, Proc. Natl. Acad. Sci. U. S. A. 106 (29) (2009) 12103–12108.

[35] T. Wang, et al., NFATc3-dependent expression of miR-153-3p promotes mitochondrial fragmentation in cardiac hypertrophy by impairing mitofusin-1 expression, Theranostics 10 (2) (2020) 553–566.

[36] H.O. Rashid, et al., ER stress: autophagy induction, inhibition and selection, Autophagy 11 (11) (2015) 1956–1977.

[37] Y. Zhang, W. Chen, Y. Wang, STING is an essential regulator of heart inflammation and fibrosis in mice with pathological cardiac hypertrophy via endoplasmic reticulum (ER) stress, Biomed. Pharmacother. 125 (2020) 110022.

[38] P. Binder, et al., Pak 2 as a novel therapeutic target for cardioprotective endoplasmic reticulum stress response, Circ. Res. 124 (5) (2019) 696–711.

[39] L.M.D. Delbridge, et al., Myocardial stress and autophagy: mechanisms and potential therapies, Nat. Rev. Cardiol. 14 (7) (2017) 412–425.

[40] Y. Zhang, J. Ren, Targeting autophagy for the therapeutic application of histone deacetylase inhibitors in ischemia/reperfusion heart injury, Circulation 129 (10) (2014) 1088–1091.

[41] E.D. Papanagnou, et al., Autophagy activation can partially rescue proteasome dysfunction-mediated cardiac toxicity, Aging Cell 21 (11) (2022) e13715.

[42] T. Oka, et al., Mitochondrial DNA that escapes from autophagy causes inflammation and heart failure, Nature 485 (7397) (2012) 251–255.

[43] K. Okada, et al., Prolonged endoplasmic reticulum stress in hypertrophic and failing heart after aortic constriction: possible contribution of endoplasmic reticulum stress to cardiac myocyte apoptosis, Circulation 110 (6) (2004) 705–712.

[44] N. Omidkhoda, et al., The role of MicroRNAs on endoplasmic reticulum stress in myocardial ischemia and cardiac hypertrophy, Pharmacol. Res. 150 (2019) 104516.

[45] J.G. Dickhout, R.E. Carlisle, R.C. Austin, Interrelationship between cardiac hypertrophy, heart failure, and chronic kidney disease: endoplasmic reticulum stress as a mediator of pathogenesis, Circ. Res. 108 (5) (2011) 629–642.

[46] M. Volpe, S. Rubattu, J. Burnett Jr., Natriuretic peptides in cardiovascular diseases: current use and perspectives, Eur. Heart J. 35 (7) (2014) 419–425.

[47] G. Gallo, et al., Natriuretic peptides: it is time for guided therapeutic strategies based on their molecular mechanisms, Int. J. Mol. Sci. 24 (6) (2023).